

Beware the Non-uniqueness of Einstein Rings

Prasenjit Saha

*Astronomy Unit, School of Mathematical Sciences
Queen Mary and Westfield College
London E1 4NS, UK*

and

Liliya L.R. Williams

*Department of Physics and Astronomy
University of Minnesota
116 Church Street SE
Minneapolis, MN 55455*

ABSTRACT

We explain how an approximation to the rings formed by the host galaxies in lensed QSOs can be inferred from the QSO data alone. A simple ring image can be made from any lens model by a simple piece of computer graphics: just plot a contour map of the arrival-time surface with closely-spaced contours. We go on to explain that rings should be (a) sensitive to time-delay ratios between different pairs of images, but (b) very insensitive to H_0 . We illustrate this for the well-known quads 1115+080 and 1608+656.

Subject headings: gravitational lensing

1. Introduction

It seems likely now that all multiple-image lens systems have Einstein rings, if imaged deep enough. Radio rings, formed out of multiply-imaged radio lobes and jets, have been known for more than a decade (Hewitt et al. 1988, Langston et al. 1990, Lehar et al. 1993). But more recently, QSO lenses when deeply imaged—especially in the infrared—have shown rings formed out of multiply-imaged parts of the QSO host galaxy: Falco et al. (1997) examined HST images of MG0414+0534 and found an arc connecting three of the four QSO images; Courbin et al. (1997) found an incipient ring in 1115+080; Impey et al. (1998) uncovered the full ring. Blandford, Surpi, & Kundić (2000, hereafter BSK) identified ring components in 1608+656.

Such a rich source of new image data is very exciting, because the paucity of constraints is a very serious problem in lens modeling, leading to large uncertainties in current lens reconstructions (see e.g., Bernstein & Fischer 1999, Williams & Saha 2000, hereafter WS). BSK and Kochanek, Keeton, & McLeod (2001, hereafter KKM) present new theoretical ideas for using ring observations to constrain lenses. In particular KKM make two very interesting points (see especially their Figure 1): (i) in a double (quad), the ring is the image of a two (four) lobed figure on the source; (ii) where a ring has brightness minima, it intersects a critical curve.

This paper presents some further theoretical work, in which we address the following question: for a lens which *already* has accurate image positions and time-delays, how much does a ring *further* constrain the lens? Our approach is very different from previous ones, and leads to some new insights: the down side is that the same ring can arise from a large range of lenses and h values, and thus the prediction by KKM that “deep, detailed observations of Einstein rings will be revolutionary for constraining mass models and determining the Hubble constant from time delay measurements” is, unfortunately over-optimistic; the up side is that rings turn out to be related to time delay measurements in an unexpected but testable way.

2. Rings and the arrival-time surface

While working on WS we noticed that a contour map of the arrival-time surface in a multiple-image system resembles a ring if the contours are very close. Figure 14 of WS shows an example. In that paper we gave a handwaving argument for why this should happen, but returning to the question afterwards led to interesting developments, which we now discuss.

The arrival-time surface produced by a source at θ_s can be expressed as

$$\tau(\theta) = 2 \nabla_{\theta}^{-2} [1 - \kappa(\theta)] - \theta \cdot \theta_s \quad (1)$$

with $\tau(\theta)$ being related to the physical arrival time¹

$$t(\theta) = H_0^{-1} (1 + z_L) \frac{d_L d_S}{d_{LS}} \tau(\theta), \quad (2)$$

where the d 's are dimensionless angular diameter distances, z_L is the lens-redshift, and $\kappa(\theta)$ the dimensionless mass profile (see e.g., equations 9 and 10 in Saha 2000). If the source is much further than the lens, then

$$t(\theta) \simeq h^{-1} z_L (1 + z_L) \times 80 \text{ days arcsec}^{-2} \tau(\theta). \quad (3)$$

If image positions, QSO time delays, redshifts, cosmology, and lens profile are all known, H_0 can be read off from equations (1) and (2). Unfortunately, this is not the case; image positions, time delays, and redshifts are accurately measurable, and cosmology produces a readily-quantifiable (and

¹We will use ‘arrival-time surface’ to refer to both $\tau(\theta)$ and $t(\theta)$, in places where this causes no ambiguity.

fairly small) uncertainty, lens profile is a large uncertainty: a large range of lens models $\kappa(\boldsymbol{\theta})$ can reproduce QSO image positions and time delay ratios exactly or nearly exactly, resulting in a range of plausible H_0 's.

An Einstein ring, being an image of an extended source, is not determined solely by the arrival-time surface for a point source, but also by the brightness distribution of the source—see e.g., equation (7) of KKM. KKM and BSK argue that not all the mass models that reproduce the QSO images will be able to reproduce the image of the QSO host galaxy. If so, it would narrow down the range of acceptable H_0 's.

How does an extended source change things? To study this, let us consider an extended source with a very simple brightness profile: peak brightness at $\bar{\boldsymbol{\theta}}_s$ and around it source brightness falling off in a conical profile

$$I_s(\bar{\boldsymbol{\theta}}_s + \Delta\boldsymbol{\theta}_s) = 1 - k |\Delta\boldsymbol{\theta}_s|. \quad (4)$$

Here k is a constant, and it is understood that where $1 - k |\dots| < 0$, the surface brightness is zero. Say one of the images of $\bar{\boldsymbol{\theta}}_s$ is at $\bar{\boldsymbol{\theta}}$ on the lens plane, and that the image-plane region $\bar{\boldsymbol{\theta}} + \Delta\boldsymbol{\theta}$ corresponds to the source-plane region $\bar{\boldsymbol{\theta}}_s + \Delta\boldsymbol{\theta}_s$. Since surface brightness is preserved, we have for the image brightness

$$I(\bar{\boldsymbol{\theta}} + \Delta\boldsymbol{\theta}) = I_s(\bar{\boldsymbol{\theta}}_s + \Delta\boldsymbol{\theta}_s) = 1 - k |\Delta\boldsymbol{\theta}_s|. \quad (5)$$

A small displacement in the source plane, $\Delta\boldsymbol{\theta}_s$, is related to the corresponding displacement in the lens plane, $\Delta\boldsymbol{\theta}$, through $\Delta\boldsymbol{\theta}_s = \mathbf{M}^{-1} \cdot \Delta\boldsymbol{\theta}$, where \mathbf{M} is the inverse magnification. With this, the illumination in the lens plane can be rewritten as

$$I(\bar{\boldsymbol{\theta}} + \Delta\boldsymbol{\theta}) = 1 - k |\mathbf{M}^{-1} \cdot \Delta\boldsymbol{\theta}|. \quad (6)$$

Now $\tau(\boldsymbol{\theta})$, the arrival time for the point source at $\boldsymbol{\theta}_s$, has zero derivative at $\bar{\boldsymbol{\theta}}$. In the neighborhood of $\bar{\boldsymbol{\theta}}_s$, the second derivatives of τ are simply \mathbf{M}^{-1} . Hence in this region, $\nabla\tau$ equals $\mathbf{M}^{-1} \cdot \Delta\boldsymbol{\theta}$. So the brightness of the ring is

$$I(\boldsymbol{\theta}) = 1 - k |\nabla\tau|. \quad (7)$$

Now picture a sheet of paper with contours of arrival time drawn on it, viewed so that nearby contour lines blur into a grayscale. Equation 7 then also happens to represent the grayscale pattern on this sheet of paper, where

$$k \propto \frac{\langle \text{thickness of contour lines} \rangle}{\langle \tau\text{-spacing between contour lines} \rangle}, \quad (8)$$

with '1' representing blank paper, and $k |\nabla\tau|$ the darkening due to the contour lines. We thus have a quantitative explanation for why Figure 14 of WS looks like a ring.

More importantly, we see that given a lens model for QSO images, generating a ring image for a conical source is very simple: one has only to plot a closely spaced contour map of the arrival-time surface; the only adjustable parameter is the contour interval, which behaves as a surrogate for the source size k^{-1} .

The relation (7) between the arrival-time surface (of the QSO or other compact source) and the ring (formed from the host galaxy) provides two insights, which are quite generic and not limited to conical sources.

1. Consider time delays versus image separations between different pairs of images in a quad. Where the ratio of time delay to image separation is small, the density of contour lines will be small, therefore the corresponding segment of the ring will be brighter. Thus, if time delay ratios in a quad have been measured then the relative brightness of different ring segments can be predicted to some extent. Conversely, if QSO images and the image of the ring are observed then time delay ratios can be estimated.
2. Altering the lens mass model, and hence $\tau(\boldsymbol{\theta})$ in such a way that there is little or no change in the density of contour lines in the region of the ring will produce little or no change in the ring (other than its overall brightness), but may cause a large change in H_0 . One example is evident from equations (1) and (2): if $[1 - \kappa(\boldsymbol{\theta})]$, $\boldsymbol{\theta}_s$, and H_0 are all multiplied by the same constant factor, $t(\boldsymbol{\theta})$ is unaffected. This is the mass-disk degeneracy, first noted by Falco et al. (1985) and discussed in several recent papers, e.g., Saha (2000); basically it means that steeper lens profile give higher H_0 from the same data—see the “radial-index versus h ” plots in WS for examples. This particular degeneracy is exact, but numerically one can cook up any number of near-degeneracies that scale H_0 significantly while producing only slight, observationally negligible, changes in rings.

In the following section we follow up the implication of these two points in detail for two quads.

3. Case studies: 1115+080 and 1608+656

These are among the most-studied lenses: 1115+080 was discovered by Weymann et al. (1980) and its time delays were determined by Schechter et al. (1997); 1608+656 was discovered by Myers et al. (1995) and Fassnacht et al. (1999) measured its time delays.

Figure 1 shows the image configurations for both lenses. We have plotted the saddle-point contours, which make up a sort of skeleton for the arrival-time surface, and renamed the images by arrival time. Upon doing this, it becomes evident how similar these two lenses are.

We can now use the ideas of the previous section to predict the morphology of the rings. The contour-density argument show that

$$\frac{(\Delta\tau_{1-3}/\Delta\theta_{1-3})}{(\Delta\tau_{2-4}/\Delta\theta_{2-4})} \approx \frac{\text{brightness of 2-4 ring segment}}{\text{brightness of 1-3 ring segment}}, \quad (9)$$

and similarly for any pair of ring segments. Now, arrival-time contours will be furthest apart in the region 2-3, closer together in 1-3 and 2-4, and closest in 1-4. So the brightest part of the ring

will be 2–3, while 1–4 will be a faint arc or a gap in the ring. The same conclusions follow from a more complicated argument based on caustics in Blandford & Kovner (1988). And they may be verified by inspecting Figure 1 of Impey et al. (1998) and Figure 1 of BSK.

We now show the predicted rings from models that precisely fit the QSO image and time-delay data. We generate ensembles of such models using the method developed in WS, with one change: instead of letting h vary in the ensemble and then examining its range, we fix it at some trial value; in this way we can examine how the predicted ring varies with the trial h . All models we show in this paper are averages of ensembles of 100. We have not attempted to fit for the contour step, we have just chosen a suitable value empirically.

Figure 2 shows a model of PG1115, for h fixed at 0.5. The model is constrained by image positions and Barkana’s (1997) estimate of the time delay from the Schechter et al. (1997) data. It predicts the gross features of the observed ring. Figure 3 is similar (h is also set to 0.5), but uses the earlier preliminary time delay estimate by Schechter et al. (1997); the only significant difference is that $\Delta t_{2,4}/\Delta t_{1,3}$ is larger, and in response the ring segment 2–4 has become fainter than 1–3. In the observed ring the 2–4 segment is actually slightly brighter than 1–3. (See Figure 1 of Impey et al. 1998, and also Figure 3 of KKM). Thus, the observed ring favors the Barkana estimate of $\Delta t_{2,4}/\Delta t_{1,3}$. Moreover, since the model is still slightly under-predicting the brightness of 2–4 versus 1–3, we further predict that as the time-delay measurements improve, $\Delta t_{2,4}/\Delta t_{1,3}$ will get somewhat smaller. This illustrates point 1 from the end of Section 2, that QSO image positions, time delay ratios, and the ring are not all independent.

The above conclusions do not depend on the trial value chosen for h . Figure 4 shows a model using the Barkana values and $h = 0.75$. The ring is similar to that in Figure 2 (Barkana values and $h = 0.5$), and demonstrates that QSO image positions and time delays determine the ring, while the mass distribution can vary substantially: compare the top right mass map in Figure 4 to that in Figure 2. This illustrates point 2 from the end of Section 2. It is also contrary to the assertion by KKM that “The Einstein ring in PG1115+080 rules out the centrally concentrated mass distributions leading to a high Hubble constant ($H_0 > 60 \text{ km s}^{-1} \text{ Mpc}$) given the measured time delays”.² Incidentally, note that the $h = 0.75$ model in Figure 4 is much more elliptical than the $h = 0.5$ model in Figure 2, but it is not much more centrally concentrated. It is easier to produce $h > 0.6$ models for this system if they are more centrally concentrated, but it is not necessary (see Figure 13 of WS).

Figures 5 and 6 are for 1608+656, and are analogous to Figures 2 and 4. The data are from Fassnacht et al. (1999) and the predicted rings may be compared with Figure 1 of BSK. Again, we find that changing h makes little difference to the ring.

Why do we, though we have no disagreement with the basic theoretical ideas in KKM, come

²KKM’s limit actually uses the preliminary Schechter et al. value for $\Delta t_{2,4}/\Delta t_{1,3}$, rather than the later Barkana value. Our argument would not change if we used the other value.

to the opposite conclusion regarding constraints on h ? The reason lies in the modeling strategy. KKM assume a fixed functional form for the lens described by a few parameters; these models have little freedom to vary radial profile, and do not allow ellipticity to vary or to twist with radius. Pixelated models, such as the ones in this paper, do not have such restrictions and thus are able to expose the degeneracies left by rings. Of course it is not necessary to use pixelated models for this purpose, parametric models with some additional parameters would also be effective. What these additional parameters need to be is not obvious, but from examining the pixelated mass maps we guess that letting the index of the radial profile vary and letting the ellipticity vary with radius are probably the most important ingredients.

4. Conclusions

We show that the arrival-time surface for a multiply-imaged QSO (or other compact source), when plotted as a contour map with densely packed contours, is approximately the lensed image of an extended source with a conical surface-brightness profile. An observed ring will depend on the source’s detailed brightness profile, so our result does not furnish a method for making detailed models of rings. However, our result does imply that the gross features of a ring are determined by the information encoded in the QSO point images alone, which leads to two useful findings, as follows.

1. It becomes possible to translate statements about time delays into statements about the ring (eq. 9). In particular, the general morphology of rings in quads becomes very easy to predict, from just the configuration of the QSO images. For the case of 1115+080, the ring can even be used to predict the sign of the current errors in the ratio of two time delays.
2. It becomes evident that the same ring can arise from a large range of mass distributions, and hence from a large range of h . The main (but not the only) contributor to this non-uniqueness is the mass disk degeneracy, which makes the lens mass profile steeper while making the Universe smaller but keeps image and time-delay data the same. We illustrate non-uniqueness in models of 1115+080 and 1608+656.

We thank J.C.B. Papaloizou for elucidating the connection between contour maps and ring images.

REFERENCES

Blandford, R.D., Surpi, G., & Kundić, T. 2000, in Brainerd, T.G. & Kochanek, C.S. Eds., “Gravitational Lensing: Recent Progress and Future Goals”, astro-ph/0001496 (BSK)

- Blandford, R.D. & Kovner, I. 1988, *Phys Rev A*, 38, 4028
- Courbin, F., Magain, P., Keeton, C.R., Kochanek, C.S., Vanderriest, C., Jaunsen, A.O., Hjorth, J., 1997, *A&A* 324, L1
- Falco, E.E., Gorenstein, M.V., & Shapiro, I.I. 1985, *ApJ* 289, L1
- Falco, E.E., Lehar, J., & Shapiro, I.I. 1997, *AJ*, 113, 540
- Fassnacht, C.D., Pearson, T.J., Readhead, A.C.S., Browne, I.W.A., Koopmans, L.V.E., Myers, S.T. & Wilkinson P.N. 1999, *ApJ*, 527, 498
- Hewitt, J.N., Turner, E.L., Schneider, D.P., Burke, B.F., Langston, G.L., & Lawrence, C.R. 1988, *Nature*, 333, 537
- Impey, C.D., Falco, E.E., Kochanek, C.S., Lehar, J., McLeod, B.A., Rix H.-W., Peng, C.Y. & Keeton, C.R. 1998, *ApJ*, 509, 551
- Kochanek, C.S., Falco, E.E., Impey, C.D., Lehar, J., McLeod, B.A., Rix, H.-W., Keeton, C.R., Muñoz, J.A., & Peng, C.Y., , 2000, *ApJ* 535, 692
- Kochanek, C.S., Keeton, C.R., McLeod, B.A. 2001, *ApJ*, 547, 50 (KKM)
- Langston, G.I., Conner, S.R. Lehar, J., Burke, B.F., & Weiler, K.W. 1990, *Nature*, 344, 43
- Lehar, J., Langston, G.I., Silber, A., Lawrence, C.R., & Burke, B.F. 1993, *AJ*, 105, 847
- Myers, S.T. et al. 1995, *ApJ*, 447, L5
- Saha, P. 2000, *AJ*, 120, 1654
- Schechter, P.L. et al. 1997, *ApJ*, 475, 85
- Weymann, R. J., Latham, D., Angel, J. R. P., Green, R. F., Liebert, J. W., Turnshek, D. A., Turnshek, D. E., & Tyson, J. A. 1980, *Nature*, 285, 641
- Williams, L.L.R. & Saha, P. 2000, *AJ* 119, 439

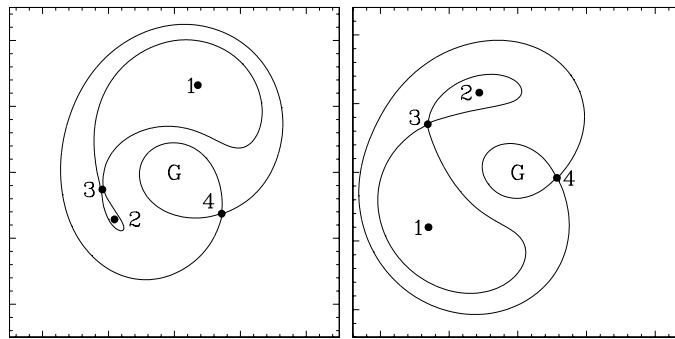


Fig. 1.— Image configuration and possible saddle-point contours on the arrival-time surface for 1115+080 and 1608+656. Images are labelled by increasing arrival time, and G labels the center of the main lensing galaxy.

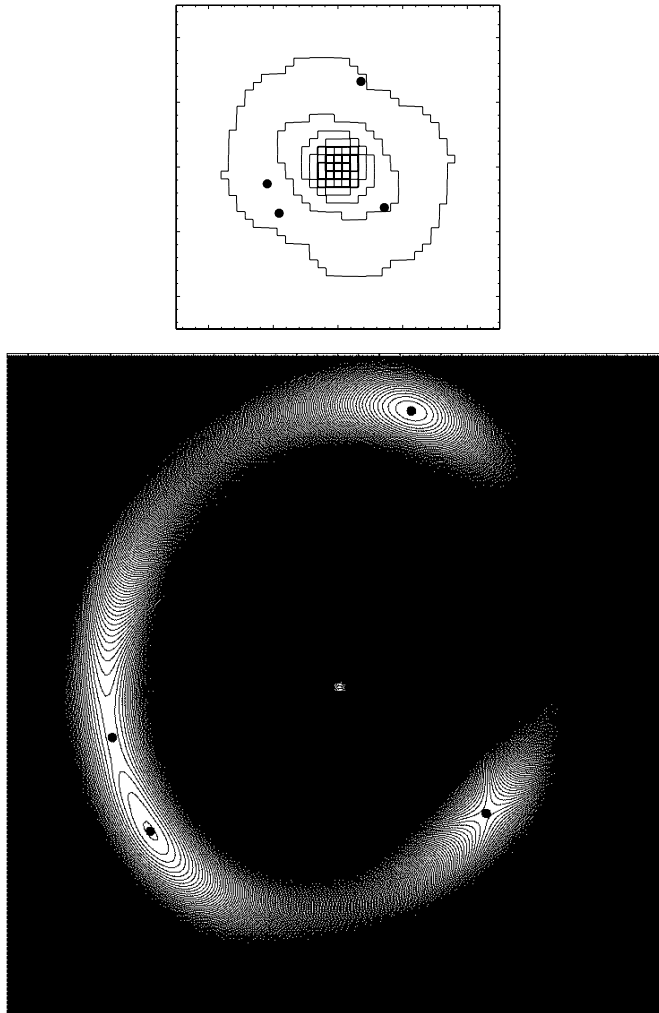


Fig. 2.— An ensemble-average model of 1115+080, constrained to give $h = 0.5$ for the Barkana (1997) estimates for the time delays. In particular the time delay ratio is $\Delta t_{2,4}/\Delta t_{1,3} = 0.88$. The upper panel is the mass map, with κ in steps of $\frac{1}{3}$. The lower panel shows the arrival-time surface with contours in spaced by 2 hr; this may be compared with the lower-left panel in Figure 1 of Impey et al. (1998).

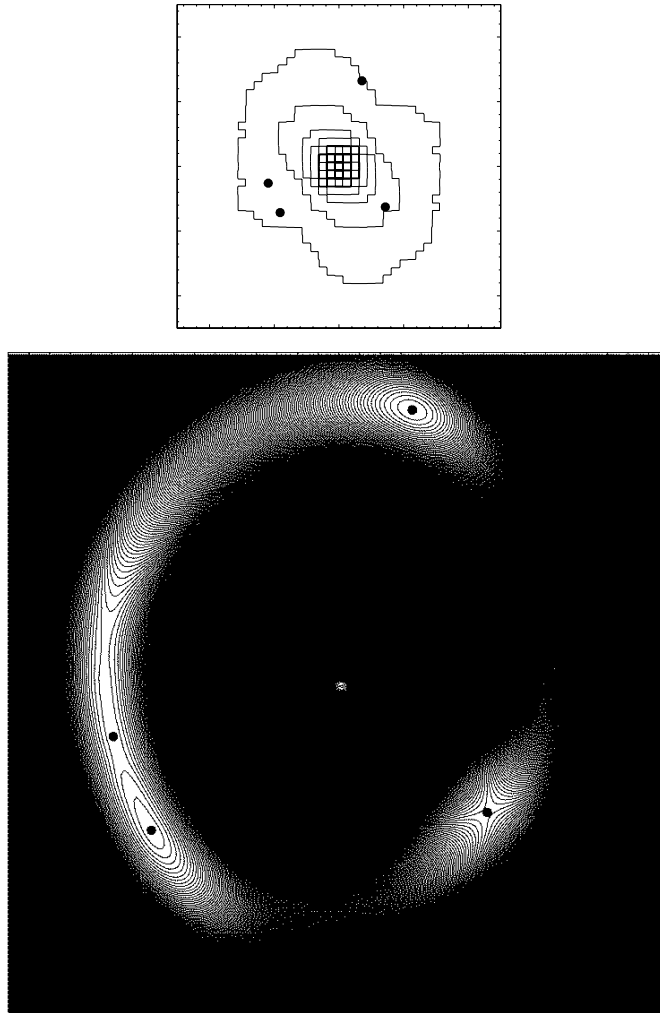


Fig. 3.— An ensemble-average model of 1115+080 constrained to give $h = 0.5$ from the Schechter et al. (1997) estimates for the time delays, in particular $\Delta t_{2,4}/\Delta t_{1,3} = 1.67$. Note how increasing $\Delta t_{2,4}/\Delta t_{1,3}$ has made the 1–3 section of the ring brighter and the 2–4 section fainter.

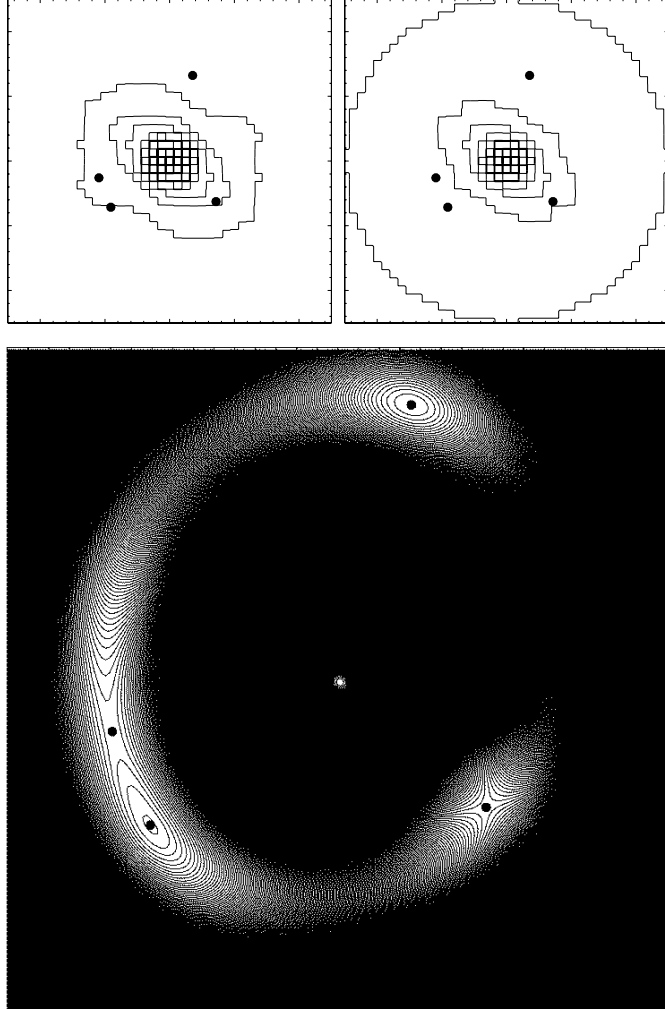


Fig. 4.— Another ensemble-average models of 1115+080, this time constrained to give $h = 0.75$ from the Barkana (1997) estimates for the time delays. The mass map is on the upper left; the upper right panel shows the mass map transformed using the mass disk degeneracy to give the same time delays for $h = 0.5$ —note that the critical-density contour (third from the outside) does not move. The $t(\theta)$ shown is identical for both mass maps.

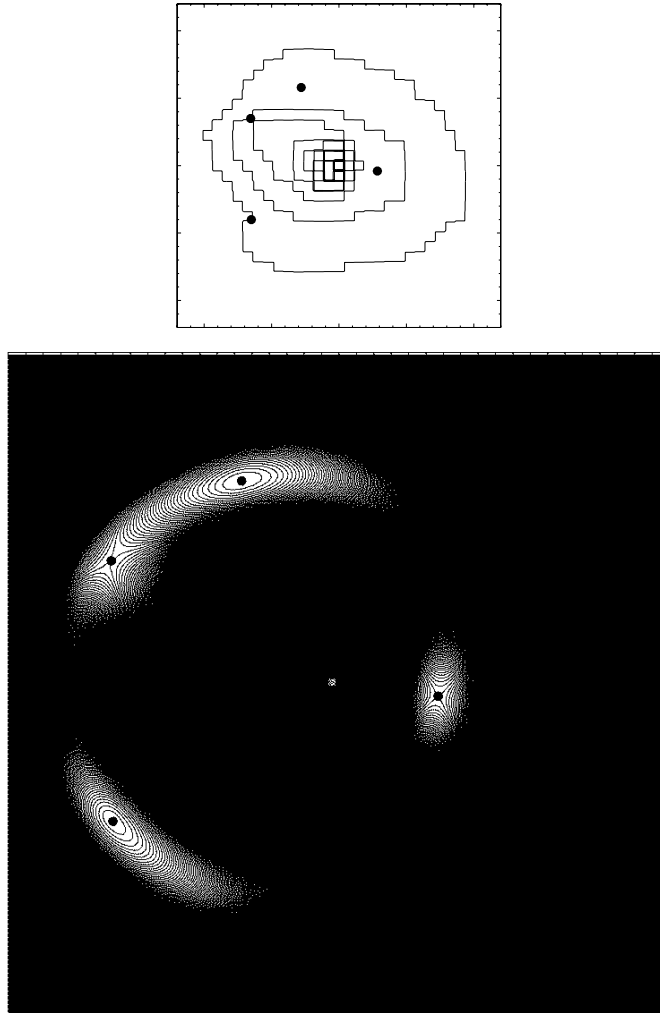


Fig. 5.— An ensemble-average model of 1608+686, constrained to give $h = 0.5$ for the Fassnacht et al. (1999) time delays. The arrival-time contours are spaced by 6 hr. The lower panel here, after rotating clockwise by 90° , may be compared with the lower-left panel in Figure 1 of BSK

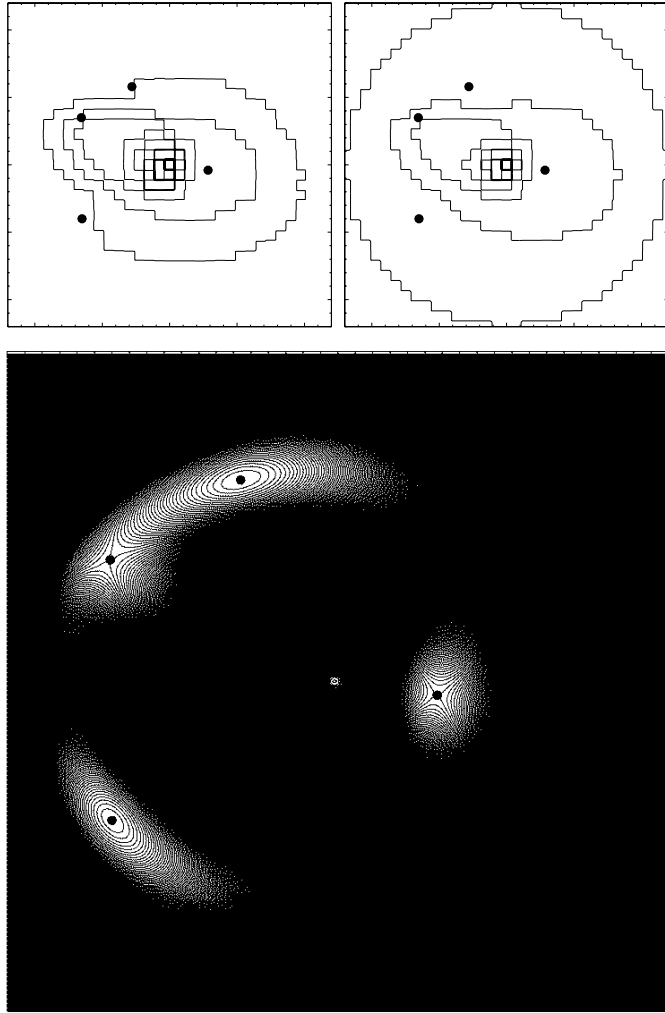


Fig. 6.— An ensemble-average model of 1608+686, constrained to give $h = 0.75$ for the Fassnacht et al. (1999) time delays. The mass map is on the upper left; the upper right panel shows the mass map transformed using the mass disk degeneracy to give the same time delays for $h = 0.5$. The ring applies to either mass map.